Materials Sciences and Applications, 2016, 7, 484-495
http://www.scirp.org/journal/msa
ISSN Online: 2153-1188
ISSN Print: 2153-117X

Synthesis and Structural Characterization of Monocrystalline α-V_2O_5 Nanowires

María Luisa Tafoya Ronquillo[1], Patricia Santiago Jacinto[1], Pilar Ovalle[1], Luis Rendón Vázquez[1], Elizabeth Chavira Martínez[2], Ernesto Marinero[3], Vicente Garibay[4]

[1]Instituto de Física, UNAM, Circuito de la Investigación s/n, Ciudad Universitaria, México, D.F., México
[2]Instituto de Investigaciones en Materiales, UNAM, Circuito de la Investigación s/n, Ciudad Universitaria, México, D.F., México
[3]Purdue University, Purdue Mall, West Lafayette, IN, USA
[4]Instituto Mexicano del Petróleo IMP, México, D.F., México
Email: tafoyamarialuisa@gmail.com

How to cite this paper: Tafoya Ronquillo, M.L., Santiago Jacinto, P., Ovalle, P., Rendón Vázquez, L., Chavira Martínez, E., Marinero, E. and Garibay, V. (2016) Synthesis and Structural Characterization of Monocrystalline α-V_2O_5 Nanowires. *Materials Sciences and Applications*, **7**, 484-495.
http://dx.doi.org/10.4236/msa.2016.79042

Received: July 29, 2016
Accepted: August 28, 2016
Published: September 1, 2016

Abstract

A stable one-dimensional system in an orthorhombic α-V_2O_5 nanowires monocrystalline structure was obtained by a solvothermal method from a polymorphic V_2O_5 structure. The starting material was firstly submitted to acid hydrolysis in H_2O_2 followed by a solvothermal treatment. The outcome of this procedure, a metastable phase of the one-dimensional system $V_{10}O_{24}{\cdot}12H_2O/V_3O_7{\cdot}H_2O$, was subsequently reoxidized by controlled heating in an open air system. The final product was an orange crystalline solid mainly formed by monocrystalline nanowires of α-V_2O_5 having lengths of tens of micrometers and widths of about 75 nm with a preferential [200] growth direction. It was found that the pH value of the initial solution plays an important role in the formation of the crystalline phase in the final products. Characterization was performed by X-ray diffraction (XRD), scanning electron microscopy (SEM) and high-resolution transmission electron microscopy (HRTEM). This study offers an alternate route for the synthesis of vanadium oxides and related compounds.

Keywords

Nanostructures, Oxides, Crystal Growth, X-Ray Diffraction, Crystal Structure

1. Introduction

One-dimensional (1D) nanostructured materials, including nanotubes, nanowires, nanobelts, nanoribbons and nanorods, often exhibit specific physical and chemical properties due to their nanometer dimensions, which differ greatly from those of their bulk counterparts [1]. Among one-dimensional structures, the synthesis of vanadium pen-

toxide (V_2O_5) and their derivative compounds has been researched intensively due to their redox activity and layered structures [2]-[11]. The layered crystal structure of V_2O_5 allows the insertion of small ions, for example Li^+ and has potential applications in lithium batteries [12]-[14], electric field-effect transistors [15] and chemical sensors or actuators [16].

Vanadium forms a variety of binary compounds with the general formula, VO_{2+x} ($-0.5 \le x \le 0.5$), such as V_2O_3, VO_2, V_2O_5, V_3O_7, V_4O_9, V_6O_{13} [17]. Among them vanadium pentoxide presents the polymorphs α-V_2O_5 (orthorhombic) [18], β-V_2O_5 (monoclinic or tetragonal) and γ-V_2O_5 (orthorhombic) structures [19] [20]. The polymorph α-V_2O_5 is one of the most widely studied transition metal oxides in the V-O system, because it is the most stable phase at atmospheric pressure and room temperature. It has a band gap of ~2.3 eV and shows a semiconductor-metal transition at about 250˚C. The α-V_2O_5 is lightly soluble in water (0.08 g/ml, 20˚C) but extremely soluble in acids. In particular it is physically and chemically stable in hot acid solutions. By increasing pressure and temperature, it is possible to improve the contact between the phases in the orthorhombic structure formed by VO_5 layers forming square pyramids that share edges and corners. In addition, the interaction between these layers is based on Van der Waals chemical bonds which favour growth of the planes along the [001] direction [21]-[23].

Nowadays, several research groups have reported the partial or total use of the solvothermal method of synthesis because it is an easy route to the formation of vanadium oxides with different morphologies [24]-[33]. In this work we synthesized by a solvothermal method at low temperature monocrystalline α-V_2O_5 nanowires with preferential [200] growth direction. In the solvothermal synthesis the oxidation states V^{5+}, V^{4+} and V^{3+} were present. The presence of V^{4+} ions in the material, promotes the growth of $V_{10}O_{24}{\cdot}12H_2O/V_3O_7{\cdot}H_2O$ nanobelts in metastable phase. However the metastable phases present in the $V_{10}O_{24}{\cdot}12H_2O/V_3O_7{\cdot}H_2O$ template are stabilized after applying a thermal process, which encourages and promotes formation of α-V_2O_5 nanowires in an orthorhombic phase. With the aid of XRD, SEM and HRTEM we have studied the morphological changes and structural behavior during the formation of α-V_2O_5 nanowires. The solvothermal chemical route seems optimal, since it is suitable for the synthesis of materials that decompose at elevated temperatures, which are poorly soluble, reactive, or for species with multiple oxidation states, as in the case of α-V_2O_5 nanowires. A benefit of this method of synthesis is that one obtains very pure products at low temperature using only V_2O_5 as starting material and hydrogen peroxide (H_2O_2) as solvent-oxidant agent. Furthermore, these α-V_2O_5 nanowires can be doped with small ions, for example Li^+ ions by electrochemical methods, and subsequently can be used as electrodes in rechargeable lithium-ion nanobatteries.

2. Experimental

2.1. Synthesis of Monocrystalline α-V_2O_5 Nanowires

The synthesis of α-V_2O_5 nanowires was performed using a solvothermal method similar

to the one reported by Guicun Li *et al.* [34]. In a typical synthesis process, 0.18 g of V_2O_5 powders (Aldrich, 99.99%) was dispersed into 30 ml of distilled with magnetic stirring (Nuova, SP18420-26Q) to form a yellow slurry solution with pH 4 (Oakton, pH/Ion 510). Then 2.5 ml of H_2O_2 (Aldrich, 30 wt%) were added drop wise to the slurry solution and stirred to 100 rpm for 5 min to form an orange solution where the pH dropped to 0.5. The solution was directly poured into an acid digestion vessel of 45 ml capacity with Teflon a liner (Parr instruments, 4744). The closed acid digestion vessel was introduced into a furnace (Lindberg/Blue M, BF81894C-1) and was maintained at 180˚C for 48 h. Once the thermal treatment was over, the furnace was turned off and left to cool to room temperature. Green precipitates were obtained at the bottom of the container, which was surrounded by a colorless solution (reduction from V^{5+} to V^{3+}). The green precipitates were collected on a paper filter, washed several times with distilled water and finally dried at room temperature for 30 h. After this, the precipitates form a film and the surface color changed from a green (V^{3+}) to a dark-blue (V^{4+}). The dark-blue layer that forms on the film of the green precipitates suggests that the end products of the solvotermal synthesis are in a metastable phase (this hypothesis was confirmed by XRD and HRTEM analysis). Finally at atmospheric pressure and starting from room temperature the metastable film was heated on a hot plate to 80˚C in treatments of 4 h and 12 h long. The crystallographic evolution of the α-V_2O_5 nanowires is presented in Figure 1. Starting with V_2O_5 in an orthorhombic phase and morphologically heterogeneous, we obtained one-dimensional structures in a metastable phase after the solvothermal synthesis due to the condensation of vanadic acid via homogeneous nucleation in the redox process and ending with α-V_2O_5 nanowires in stable orthorhombic phase formed via dehydration of the one-dimensional structures in metastable phase.

2.2. Structural Characterization

X-ray diffraction analysis (XRD) was performed using a D8-Advanced Bruker

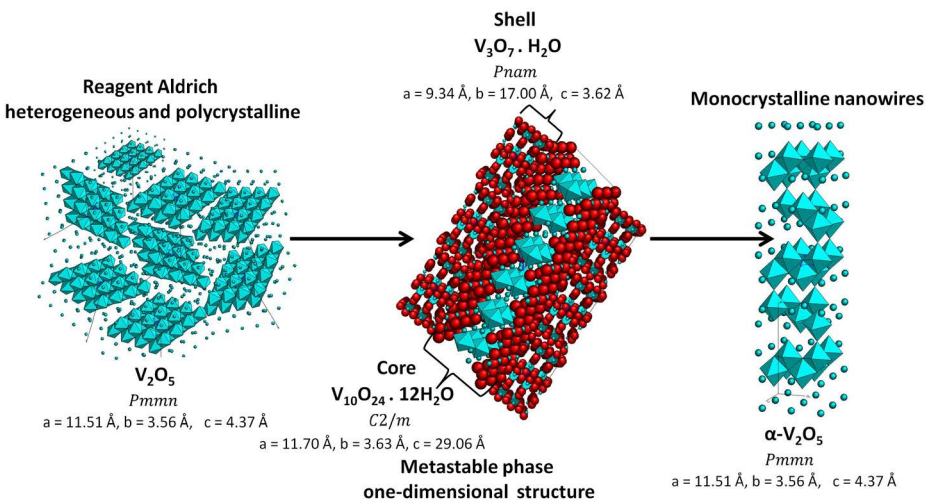

Figure 1. Simulation CaRIne V.3.1 of the synthesis of α-V_2O_5 nanowires.

diffractometer with CuKα monochromatic radiation (λ = 1.5405 Å, 2θ) using a Bragg-Brentano geometry. The samples for this analysis were subjected to slight mechanical milling. The XRD was refined using the Rietveld method and the FULLPROF program. The size of the structure was determined by the Debye Scherrer method. The morphological characterization of the products was studied by Scanning Electron Microscopy (SEM) with a microscope JEOL model JSM 7600F equipped with tungsten filament, operating at 20 kV and a pressure of 20 Pa and using the backscattered electron signal. For SEM analysis, the samples were directly placed on a specimen carrier and without adding any conductive layer. The High-Resolution Transmission Electron Microscopy (HRTEM) was done with a TITAN 80 - 300 microscope operating in the 80 - 300 kV range and a Tecnai G2-F30 operating at 300 kV. For the HRTEM observations, mechanically milled samples were deposited on the surface of a copper grid, previously coated with carbon and fomvar films.

3. Results and Discussion

XRD patterns and SEM images obtained from the samples show the structural and morphological changes during the synthesis of the α-V_2O_5 nanowires. In the Figure 2, the SEM images correspond to each of the patterns of X-ray diffraction of the samples in different reaction times. As shown by SEM, the V_2O_5 reagent (Aldrich) is formed by agglomerates of morphologically heterogeneous grains with sizes 62.46 nm - 816.73 nm. In this case, the reflections in the XRD pattern (Figure 2(a)), are indexed as V_2O_5 in orthorhombic phase (PDF 41-1426). The precipitates dried at room temperature for 30 h obtained after solvothermal synthesis at 180˚C for 48 h, XRD patterns show that the metastable film green-blue (V^{3+}/V^{4+}) is a mixture of vanadium oxides in different phases (Figure 2(b)).

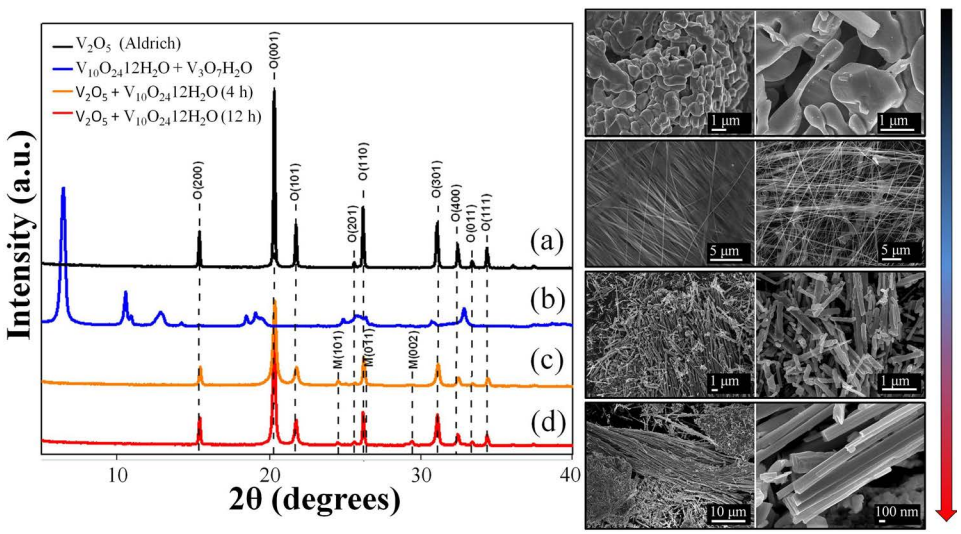

Figure 2. XRD patterns and SEM images of vanadium oxide synthesized by solvothermal method at 180˚C for 48 h. (a) V_2O_5 reagent (Aldrich), (b) $V_{10}O_{24}{\cdot}12H_2O/V_3O_7{\cdot}H_2O$ in metastable phase, (c) after the thermal process for 4 h, (d) after the thermal process for 12 h.

The XRD patterns refined by Rietveld (Figure 3), determine that the metastable film is constituted by 66% of $V_{10}O_{24}{\cdot}12H_2O$ in monoclinic phase (Figure 3(a)) with lattice parameters a = 11.70 Å, b = 3.63 Å and c = 29.06 Å (PDF 25-1006). In addition this analysis shows that the other 34% present in the metastable film, corresponds to the $V_3O_7{\cdot}H_2O$ oxide in orthorhombic phase (Figure 3(b)) with lattice parameters a = 9.34 Å, b = 17.00 Å and c = 3.62 Å (PDF 28-1433). SEM images shown that the bi-compound template of $V_{10}O_{24}{\cdot}12H_2O/V_3O_7{\cdot}H_2O$ is conformed by overlapping nanobelts, growing both on the surface and in the inside of the film. These one-dimensional structures have an average width of 209.55 nm and hundreds of micrometers long.

The color of the metastable $V_{10}O_{24}{\cdot}12H_2O/V_3O_7{\cdot}H_2O$ film (monoclinic and orthorhombic, respectively) changes from green-blue to yellow-pale after a thermal process at 80˚C at atmospheric pressure for 4 h, which causes the oxidation of the products to V^{5+} and the stabilization partial of the phases. The XRD pattern (Figure 2(c)) shows reflections corresponding to a 92.8% V_2O_5 in orthorhombic phase (α-V_2O_5), with lattice parameters a = 11.51 Å, b = 3.56 Å and c = 3.22 Å, indexed in agreement to the PDF 41-1426. However, we see the reflections due to the remnant of the $V_{10}O_{24}{\cdot}12H_2O$ in monoclinic phase (PDF 25-1006). The smaller interplanar spacing is caused by the removal of water from the interlamellar region of $V_{10}O_{24}{\cdot}12H_2O/V_3O_7{\cdot}H_2O$ structure. SEM images show homogeneous α-V_2O_5 nanowires measuring in average 111.90 nm in cross section and hundreds of micrometers long. After increasing the thermal process to 12 h, the color in the metastable film change from green-blue to orange, indicating the progress of oxidation state V^{5+} in the material. The intensity of the diffractions peaks associated α-V_2O_5 in stable orthorhombic phase increased with 95.8% of (Figure 2(d)) and clearly decreased by 4.2% the reflections associated to $V_{10}O_{24}{\cdot}12H_2O$ in metastable monoclinic phase. The crystal structures of the α-V_2O_5 nanowires are similar to that of the commercial V_2O_5 powders (Figure 2(a)).

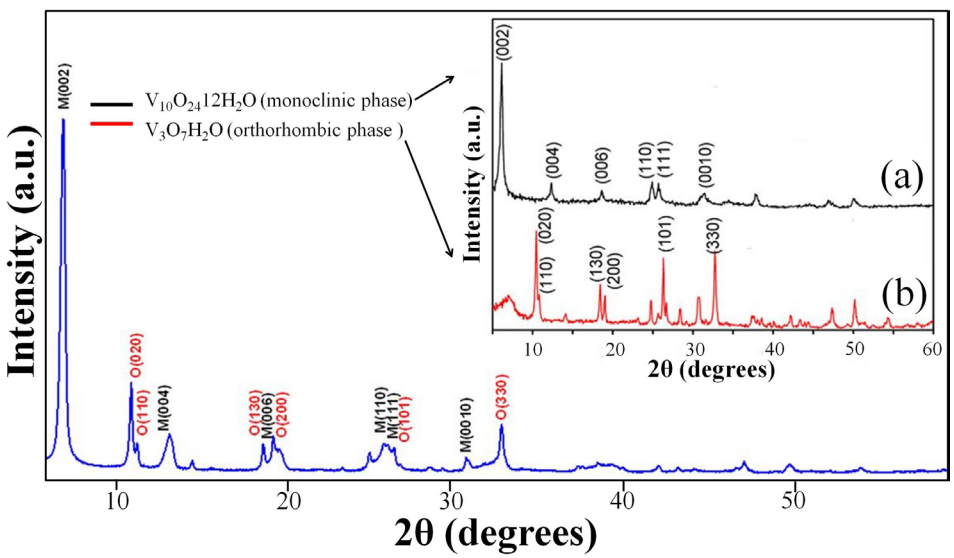

Figure 3. XRD pattern refined by Rietveld of metastable phase. (a) $V_{10}O_{24}{\cdot}12H_2O$ monoclinic phase; (b) $V_3O_7{\cdot}H_2O$ orthorhombic phase.

A probable process for the observed evolution of morphologies and crystal structures can be understood as follows: the process begins when vanadium salts are dissolved partially in distilled water; the metal cations (V^{5+}) are solvated by molecules of water and the proposed reaction is (Equation (1)):

$$V_2O_5 + H_2O \rightarrow V_2O_5nH_2O \quad (1)$$

For transition metal cations, charge transfer occurs from the σ orbitals of the water molecule to the empty metal d orbitals, this causes an increase in the acidity of the water [35]. The molecule is dissociating by the acid hydrolysis caused by the addition of H_2O_2. Therefore, the degree of acid hydrolysis is controlled by pH 0.5 in the precursor phase solution (Equation (2)).

$$V_2O_5nH_2O + H_2O_2 \rightarrow 2H_3VO_4 \quad (2)$$

The electron transfer increases the charge on the molecule and weakens the OH bonds [36]-[39]. Applying pressure and temperature, monoperoxo and dimer species are then progressively formed as peroxo groups are decomposed (Equation (3)).

$$2H_3VO_4 \rightarrow VO_2^+ + VO_2^+ + OH^- \quad (3)$$

The system redox efficiently promotes a molecular rearrangement due to the condensation of vanadic acid via a homogeneous nucleation into the reduction of V^{5+} ions to V^{3+} ions, resulting in a metastable crystalline structure $V_{10}O_{24}{\cdot}12H_2O$ (hydrated bariandite) in monoclinic phase with one-dimensional growth (Equation (4)).

$$8VO_2^+ + 2VO_2^+ + 12OH^- \rightarrow V_{10}O_{24}\cdot 12H_2O \quad (4)$$

The partial stability of these products in metastable phase is achieved naturally when oxidized by exposure to air in the process of washing and drying (partially oxidation of V^{3+} to V^{4+} ions), obtaining as final products, a mixture of vanadium oxide in different phase but with an one-directional growth (Equation (5)).

$$V_{10}O_{24}\cdot 12H_2O \rightarrow V_{10}O_{24}\cdot 12H_2O + V_3O_7\cdot H_2O_{sup} \quad (5)$$

With the thermal process of 4 and 12 h the phases in the metastable products $V_{10}O_{24}{\cdot}12H_2O/V_3O_7{\cdot}H_2O$ are stabilized removing the un-coordinated water molecules with metal centers V-O, giving rise to structures of V_2O_5 nanowires in stable orthorhombic phase (Equation (6)).

$$V_{10}O_{24}\cdot 12H_2O + V_3O_7\cdot H_2O_{sup} \rightarrow V_2O_5 \quad (6)$$

The HRTEM micrographs (**Figure 4**), show the variety of one-dimensional structures forming the metastable phase $V_{10}O_{24}{\cdot}12H_2O/V_3O_7{\cdot}H_2O$ template. These bi-compound nanobelts exhibit an average width of 125 - 250 nm and in some cases are core-shell types. On the other hand it is determined that the shell is not uniform in all cases; furthermore, it varies along the same nanobelt, which clearly indicates a non- uniform oxidation.

It is determined that the shell is constituted by the $V_3O_7{\cdot}H_2O$ oxide in orthorhombic phase with families of planes {200}, {200}, {101}, {230}, {120} and interplanar distances of 0.850 nm, 0.467 nm, 0.339 nm, 0.360 nm, 0.630 nm respectively (**Figure 5**).

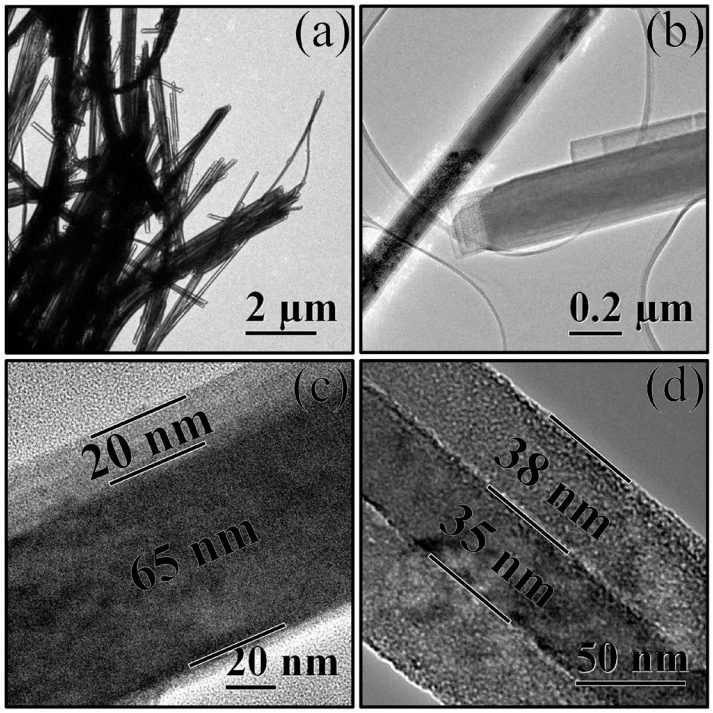

Figure 4. TEM images of the $V_{10}O_{24}{\cdot}12H_2O/V_3O_7{\cdot}H_2O$ template in metastable phase. (a) Distribution to low-magnification; (b) Metastables structures to high-magnification; (c) and (d) Bi-compound nanobelts type core-shell.

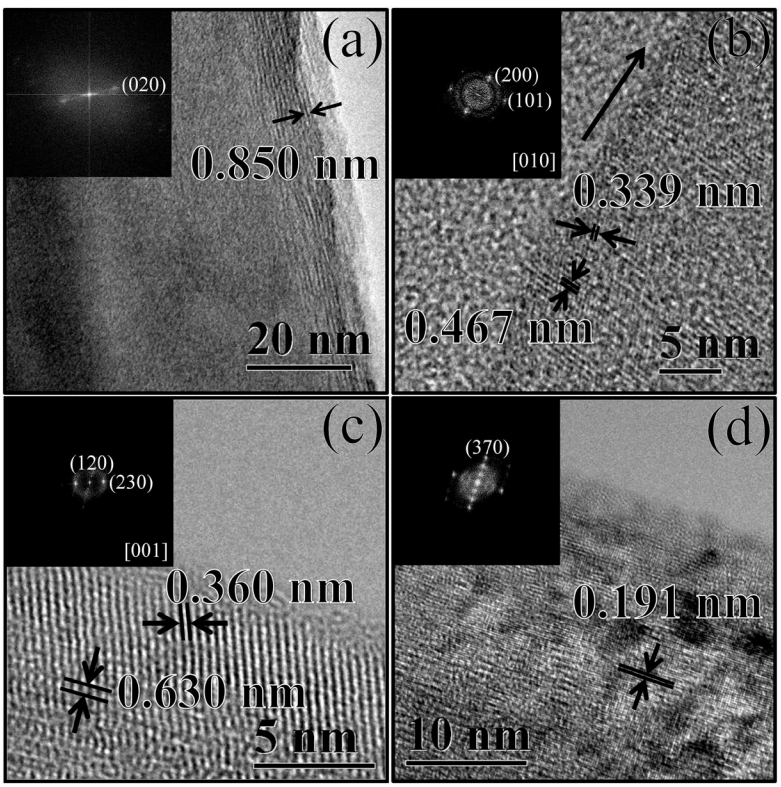

Figure 5. HRTEM images of $V_3O_7{\cdot}H_2O$ shell.

In the same way is established that the core corresponds to $V_{10}O_{24}{\cdot}12H_2O$ in monoclinic phase which exhibits the families of planes {004}, {317} and {313} with *d*-spacing of 0.708 nm, 0.236 nm and 0.245 nm respectively (Figure 6). These results are consistent with those established by the XRD patterns corresponding to the analysis in the metastable phase.

With the thermal processes of 4 and 12 h the metastable phases in the one-dimensional $V_{10}O_{24}{\cdot}12H_2O/V_3O_7{\cdot}H_2O$ template are stabilized. The crystal structure corresponds to an orthorhombic phase, obtaining α-V_2O_5 nanowires monocrystalline that are morphologically stable at atmospheric pressure and room temperature. As result the α-V_2O_5 nanowires are monocrystalline, they have families of planes {200}, {310}, {110}, with *d*-spacing of 0.576 nm, 0.340 nm and 0.261 nm, respectively (Figure 7).

4. Conclusion

We have obtained monocrystalline nanowires of α-V_2O_5 in orthorhombic phase by a low temperature using a solvothermal synthesis, inducing a redox process controlled in the V_2O_5 reagent grade and morphologically heterogeneous. These one-dimensional α-V_2O_5 structures have lengths of tens of micrometers and widths of about 75 nm, with a preferential [200] growth direction. Into the solvothermal synthesis, the formation of α-V_2O_5 nanowires is promoted by a template conformed of $V_{10}O_{24}{\cdot}12H_2O/V_3O_7{\cdot}H_2O$

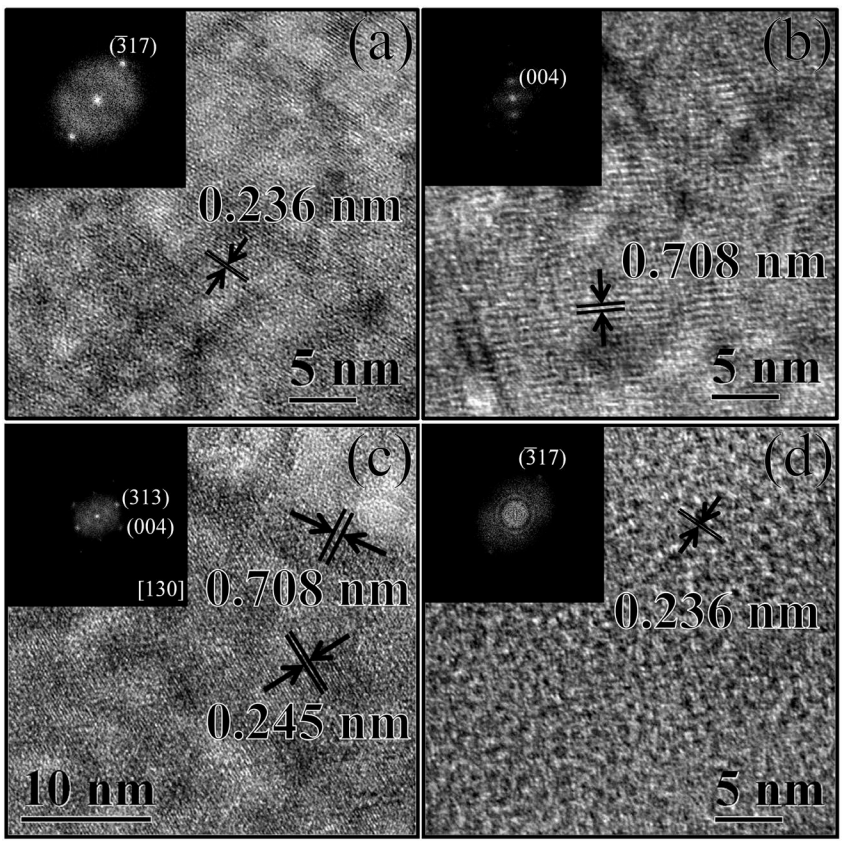

Figure 6. HRTEM images of $V_{10}O_{24}{\cdot}12H_2O$ core.

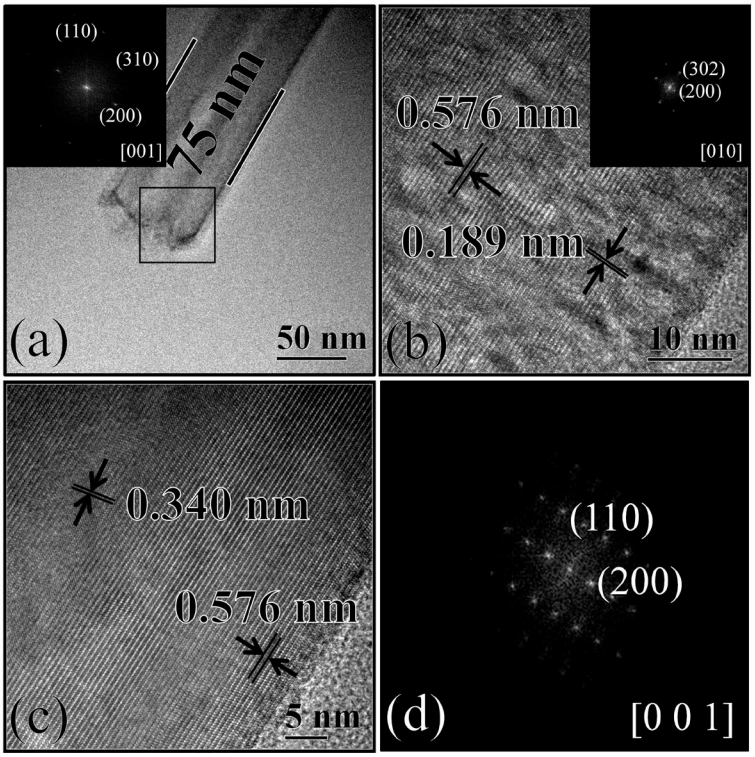

Figure 7. HRTEM images of α-V_2O_5 nanowires 12 h.

nanobelts in metastable phase. In addition, formation of $V_{10}O_{24}{\cdot}12H_2O/V_3O_7{\cdot}H_2O$ nanobelts in metastable phase depends strongly on the reaction conditions, like pH of the phase precursor solution, temperature into the acid digestion vessel, along with the time of the solvotermal reaction. It is determined that the bi-compound system in metastable phase may present core-shell type structures with average widths 209.55 nm and hundreds of micrometers long. Furthermore, the analysis presented identified the $V_{10}O_{24}{\cdot}12H_2O$ in monoclinic phase as the core, and the orthorhombic phase $V_3O_7{\cdot}H_2O$ as the shell. A thermal process stabilized metastable phases in the products in periods of 4 and 12 h. The influence of the time in the thermal process has a direct impact on the morphologies of the monocrystalline α-V_2O_5 nanowires, which have wide applications in lithium-ion batteries.

Acknowledgements

We acknowledge the financial support CONACYT Nº 311298 and PAPIIT Nº IN113411. The authors are also thankful to Laboratory of Microscopy facilities of the Mexican Petroleum Institute (IMP) and Crystal Structures Refinement Laboratory (LAREC) facilities of the Institute of Physics, UNAM and particularly to M. C. Manuel Aguilar for the XRD measurements.

References

[1] Alivisatos, A.P. (1996) Semiconductor Clusters, Nanocrystals, and Quantum Dots. *Science*,

271, 933-937. http://dx.doi.org/10.1126/science.271.5251.933

[2] Liu, J., Li, Q., Wang, T., Yu, D. and Li, Y. (2004) Metastable Vanadium Dioxide Nanobelts: Hydrothermal Synthesis, Electrical Transport, and Magnetic Properties. *Angewandte Chemie International Edition in English*, **43**, 5048-5052. http://dx.doi.org/10.1002/anie.200460104

[3] Phetmung, H., Kim, T.W., Hwang, S.J. and Choy, J.H. (2008) A Simple and Direct Method for Synthesis of Vanadium Oxide Ribbon-Like Manobelts. *Journal of the Iranian Chemical Society*, **5**, 706-711. http://dx.doi.org/10.1007/BF03246153

[4] Wu, X., Tao, Y., Dong, L. and Hong, J. (2004) Synthesis and Characterization of Self- Assembling $(NH_4)_{0.5}V_2O_5$ Nanowires. *Journal of Materials Chemistry*, **14**, 901. http://dx.doi.org/10.1039/b314775d

[5] Liu, J., Wang, X., Peng, Q. and Li, Y. (2005) Vanadium Pentoxide Nanobelts: Highly Selective and Stable Ethanol Sensor Materials. *Advanced Materials*, **17**, 764-767. http://dx.doi.org/10.1002/adma.200400993

[6] Lavayen, V., O'Dwyer, C., Santa Ana, M.A., Newcomb, S.B., Benavente, E., González, G., *et al.* (2006) Comparative Structural-Vibrational Study of Nano-Urchin And Nanorods of Vanadium Oxide. *Physica Status Solidi*, **243**, 3285-3289. http://dx.doi.org/10.1002/pssb.200669107

[7] Aghabozorg, H.R., Mousavi, R., Asckari, S. and Aghabozorg, H. (2007) Effects of Synthesis Methods of Vanadium Oxide Nanotubes on the Inter Layer Distances. *Journal of Nanoparticle Research*, **9**, 497-500. http://dx.doi.org/10.1007/s11051-006-9072-y

[8] Nguyen, T.-D. and Do, T.-O. (2013) ChemInform Abstract: Size and Shap-Controlled Synthesis of Monodisperse Metal Oxide and Mixed Oxide Nanocrystals. *ChemInform*, **44**. http://dx.doi.org/10.1002/chin.201340211

[9] Lutta, S.T., Dong, H., Zavalij, P.Y. and Whittingham, M.S. (2005) Synthesis of Vanadium Oxide Nanofibers and Tubes Using Polylactide Fibers as Template. *Materials Research Bulletin*, **40**, 383-393. http://dx.doi.org/10.1016/j.materresbull.2004.10.005

[10] Chine, M.K., Sediri, F. and Gharbi, N. (2011) Hydrothermal Synthesis of $V_3O_7{\cdot}H_2O$ Nanobelts and Study of Their Electrochemical Properties. *Materials Sciences and Applications*, **2**, 964-970. http://dx.doi.org/10.4236/msa.2011.28129

[11] Li, G., Pang, S., Wang, Z., Peng, H. and Zhang, Z. (2005) Synthesis of $H_2V_3O_8$ Single-Crystal Nanobelts. *European Journal of Inorganic Chemistry*, **2005**, 2060-2063. http://dx.doi.org/10.1002/ejic.200400967

[12] Trikalitis, P.N., Petkov, V. and Kanatzidis, M.G. (2003) Structure of Redox Intercalated $(NH_4)_{0.5}V_2O_5{\cdot}mH_2O$ Xerogel Using the Pair Distribution Function Technique. *Chemistry of Materials*, **15**, 3337-3342. http://dx.doi.org/10.1021/cm030173y

[13] Chou, S., Wang, J., Sun, J., Wexler, D., Forsyth, M., Liu, H., *et al.* (2008) High Capacity, Safety, and Enhanced Cyclability of Lithium Metal Battery Using a V_2O_5 Nanomaterial Cathode and Room Temperature Ionic Liquid Electrolyte. *Chemistry of Materials*, **20**, 7044-7051. http://dx.doi.org/10.1021/cm801468q

[14] Wang, Y., Takahashi, K., Lee, K.H. and Cao, G.Z. (2006) Nanostructured Vanadium Oxide Electrodes for Enhanced Lithium-Ion Intercalation. *Advanced Functional Materials*, **16**, 1133-1144. http://dx.doi.org/10.1002/adfm.200500662

[15] Kim, G.T., Muster, J., Krstic, V., Park, J.G., Park, Y.W., Roth, S., *et al.* (2000) Field-Effect Transistor Made of Individual V_2O_5 Nanofibers. *Applied Physics Letters*, **76**, 1875-1877.

[16] Biette, L., Carn, F., Maugey, M., Achard, M.-F., Maquet, J., Steunou, N., *et al.* (2005) Macroscopic Fibers of Oriented Vanadium Oxide Ribbons and Their Application as Highly

Sensitive Alcohol Microsensors. *Advanced Materials*, **17**, 2970-2974. http://dx.doi.org/10.1002/adma.200501368

[17] Katzke, H., Tolédano, P. and Depmeier, W. (2003) Theory of Morphotropic Transformations in Vanadium Oxides. *Physical Review B*, **68**, 024109. http://dx.doi.org/10.1103/PhysRevB.68.024109

[18] Singh, P. and Kaur, D. (2008) Influence of Film Thickness on Texture and Electrical and Optical Properties of Room Temperature Deposited Nanocrystalline V_2O_5 Thin Films. *Journal of Applied Physics*, **103**, 043507. http://dx.doi.org/10.1063/1.2844438

[19] Su, Q., Lan, W., Wang, Y.Y. and Liu, X.Q. (2009) Structural Characterization of β-V_2O_5 Films Prepared by DC Reactive Magnetron Sputtering. *Applied Surface Science*, **255**, 4177-4179. http://dx.doi.org/10.1016/j.apsusc.2008.11.002

[20] Balog, P., Orosel, D., Cancarevic, Z., Schön, C. and Jansen, M. (2007) V_2O_5 Phase Diagram Revisited at High Pressures and High Temperatures. *Journal of Alloys and Compounds*, **429**, 87-98. http://dx.doi.org/10.1016/j.jallcom.2006.04.042

[21] Londero, E. and Schröder, E. (2010) Role of van der Waals Bonding in the Layered Oxide V_2O_5: First-Principles Density-Functional Calculations. *Physical Review B*, **82**, 054116. http://dx.doi.org/10.1103/PhysRevB.82.054116

[22] Haber, J., Witko, M. and Tokarz, R. (1997) Vanadium Pentoxide I. Structures and Properties. *Applied Catalysis A*: *General*, **157**, 3-22. http://dx.doi.org/10.1016/S0926-860X(97)00017-3

[23] Enjalbert, R. and Galy, J. (1986) A Refinement of the Structure of V_2O_5. *Acta Crystallographica Section C*: *Structural Chemistry*, **42**, 1467-1469. http://dx.doi.org/10.1107/S0108270186091825

[24] Li, G., Chao, K., Peng, H., Chen, K. and Zhang, Z. (2007) Low-Valent Vanadium Oxide Nanostructures with Controlled Crystal Structures and Morphologies. *Inorganic Chemistry*, **46**, 5787-5790. http://dx.doi.org/10.1021/ic070339n

[25] Vieira, N.C., Avansi, W., Figueiredo, A., Ribeiro, C., Mastelaro, V.R. and Guimarães, F.E. (2012) Ion-Sensing Properties of 1D Vanadium Pentoxide Nanostructures. *Nanoscale Research Letters*, **7**, 310. http://dx.doi.org/10.1186/1556-276X-7-310

[26] Nanotubes, V.O., Distribution, E.B. and Iv, N.M. (2001) Defense Technical Information Center Compilation Part Notice.

[27] Kulova, T.L., Skundin, A.M., Balakhonov, S.B., Semenenko, D.A., Pomerantseva, E.A., Veresov, A.G., *et al*. (2011) Study of Electrochemical Lithium Incorporation to Whisker Structure Based on Barium-Vanadium Bronze $BaV_8O_{21-\delta}$. *Protection of Metals*, **44**, 39-42. http://dx.doi.org/10.1134/S0033173208010049

[28] McNulty, D., Buckley, D.N. and O'Dwyer, C. (2014) Polycrystalline Vanadium Oxide Nanorods: Growth, Structure and Improved Electrochemical Response as a Li-Ion Battery Cathode Material. *Journal of the Electrochemical Society*, **161**, A1321-A1329. http://dx.doi.org/10.1149/2.0601409jes

[29] Pavasupree, S., Suzuki, Y., Kitiyanan, A., Pivsa-Art, S. and Yoshikawa, S. (2005) Synthesis and Characterization of Vanadium Oxides Nanorods. *Journal of Solid State Chemistry*, **178**, 2152-2158. http://dx.doi.org/10.1016/j.jssc.2005.03.034

[30] Dexmer, J., Leroy, C.M., Binet, L., Heresanu, V., Launois, P., Steunou, N., *et al*. (2008) Vanadium Oxide-PANI Nanocomposite-Based Macroscopic Fibers: 1D Alcohol Sensors Bearing Enhanced Toughness. *Chemistry of Materials*, **20**, 5541-5549. http://dx.doi.org/10.1021/cm800886v

[31] Nguyen, T.-D. and Do, T.-O. (2009) Solvo-Hydrothermal Approach for the Shape-Selective

Synthesis of Vanadium Oxide Nanocrystals and Their Characterization. *Langmuir*, **25**, 5322-5332. http://dx.doi.org/10.1021/la804073a

[32] Livage, J. (2010) Hydrothermal Synthesis of Nanostructured Vanadium Oxides. *Materials* (*Basel*), **3**, 4175-4195. http://dx.doi.org/10.3390/ma3084175

[33] Mai, L.Q., Lao, C.S., Hu, B., Zhou, J., Qi, Y.Y., Chen, W., *et al*. (2006) Synthesis and Electrical Transport of Single-Crystal $NH_4V_3O_8$ Nanobelts. *The Journal of Physical Chemistry B*, **110**, 18138-18141. http://dx.doi.org/10.1021/jp0645216

[34] Li, G., Pang, S., Jiang, L., Guo, Z. and Zhang, Z. (2006) Environmentally Friendly Chemical route to Vanadium Oxide Single-Crystalline Nanobelts as a Cathode Material for Lithium-Ion Batteries. *The Journal of Physical Chemistry B*, **110**, 9383-9386. http://dx.doi.org/10.1021/jp060904s

[35] Schindler, M., Hawthorne, F.C. and Baur, W.H. (2000) Crystal Chemical Aspects of Vanadium: Polyhedral Geometries, Characteristic Bond Valences, and Polymerization of (VO_n) Polyhedra. *Chemistry of Materials*, **12**, 1248-1259. http://dx.doi.org/10.1021/cm990490y

[36] Fernández de Luis, R., Mesa, J.L., Urtiaga, M.K., Lezama, L., Arriortua, M.I. and Rojo, T. (2008) Topological Description of a 3D Self-Catenated Nickel Hybrid Vanadate Ni(bpe)$(VO_3)_2$. Thermal Stability, Spectroscopic and Magnetic Properties. *New Journal of Chemistry*, **32**, 1582-1589. http://dx.doi.org/10.1039/b800820e

[37] Li, B., Xu, Y., Rong, G., Jing, M. and Xie, Y. (2006) Vanadium Pentoxide Nanobelts and Nanorolls: From Controllable Synthesis to Investigation of Their Electrochemical Properties and Photocatalytic Activities. *Nanotechnology*, **17**, 2560-2566. http://dx.doi.org/10.1088/0957-4484/17/10/020

[38] Zhang, S., Shang, B., Yang, J., Yan, W., Wei, S. and Xie, Y. (2011) From VO_2 (B) to VO_2 (A) Nanobelts: First Hydrothermal Transformation, Spectroscopic Study and First Principles Calculation. *Physical Chemistry Chemical Physics*, **13**, 15873-158781. http://dx.doi.org/10.1039/c1cp20838a

[39] Maganas, D., Roemelt, M., Hävecker, M., Trunschke, A., Knop-Gericke, A., Schlögl, R., *et al*. (2013) First Principles Calculations of the Structure and V L-Edge X-Ray Absorption Spectra of V_2O_5 Using Local Pair Natural Orbital Coupled Cluster Theory and Spin-Orbit Coupled Configuration Interaction Approaches. *Physical Chemistry Chemical Physics*, **15**, 7260-7276. http://dx.doi.org/10.1039/c3cp50709b